

## *Modeling and numerical simulation of E. coli dynamics in water body*

## *Modelagem e simulação numérica da dinâmica de E. coli em corpo hídrico*

Dennis da Silva Ferreira<sup>1</sup>; Warlyton Silva Martins<sup>2</sup>;  
Grasiele Soares Cavallini<sup>3</sup>; Douglas Azevedo Castro<sup>4</sup>

### **Abstract**

This article discusses the importance of monitoring water quality in public health and use of mathematical modeling to predict environmental impact. For monitoring, the *E. coli* indicator was chosen, and a one-dimensional hydrodynamic equation was used for mathematical simulation, which was solved using the Crank-Nicolson method. The results of the mathematical model and developed algorithm were validated according to data from the literature.

**Keywords:** Mathematical modeling; contamination bioindicators; environmental monitoring.

### **Resumo**

Este artigo discorre sobre a importância do monitoramento da qualidade da água na saúde pública e a utilização da modelagem matemática para previsão de impactos ambientais. Para o monitoramento foi escolhido o indicador *E. coli* e utilizado para simulação matemática uma equação hidrodinâmica unidimensional que foi solucionada pelo método de Crank-Nicolson. Os resultados do modelo matemático e o algoritmo desenvolvidos foram validados pela literatura.

**Palavras-chave:** Modelagem matemática; bioindicadores de contaminação; monitoramento ambiental.

<sup>1</sup> PhD student, Dept. Chemistry, UFSCar, SP, Brazil; E-mail: dennis-ferreira10@hotmail.com

<sup>2</sup> PhD student, Depto. Plant Production, UFT, Gurupi, TO, Brazil, E-mail: warlytonsilva@gmail.com

<sup>3</sup> Prof. Dr., Depto. Chemistry and Plant Production, UFT, Gurupi, TO, Brazil, E-mail: grasiele@uft.edu.br

<sup>4</sup> Prof. Dr., Depto. Chemistry, UFT, Gurupi, TO, Brazil, E-mail: dcastro@uft.edu.br

## Introduction

Intense human changes in water resources have hindered their management, in terms of various environmental degradation factors, various social, economic, environmental, and technological changes, and uncertainties concerning future of water resources (SEFFRIN, 2001).

Mathematical modeling favors predictive and understanding studies of phenomena, such as predictions regarding the physical-chemical and biological characteristics of water bodies, and can thus be considered a support tool in studies and decision-making related to environmental impact (BASSANEZI, 2002).

In particular, in the management of water bodies, mathematical and computational modeling is a powerful tool, as it can simulate empirical situations by analyzing remote and imminent scenarios of the most diverse phenomena (CLIVERD *et al.*, 2016).

The use of these computational resources associated with mathematical modeling is a complex problem solver in environmental management and water engineering. Note that these mathematical applications in water systems can manage resources in a manner compatible with the assimilation potentials of water bodies, in addition to effluent release patterns, and with classifying water bodies into a use class and licensing a potentially suspected pollution activity (BALDOCHI, 2002; TUNDISI, 2021).

Therefore, mathematical modeling applied to hydrodynamics is a tool of extreme importance for managing water resources, but its use is still limited to the different methods of obtaining information about the behavior of the system, which invites adaptations both in present and future scenarios, because its limiting character affects the ability of the models to present the quality of the modeled results in a real and precise manner (JOBIM, 2012).

For the evaluation of water bodies contaminated by sewage, the most used parameters concern the presence of microorganisms with pathogenic potential and *Escherichia coli* (*E. coli*), a direct environmental indicator of fecal contamination and easy resistance to the main antimicrobials (OSINSKA *et al.*, 2016). In addition, it is a microorganism that can be isolated in various places in the human body, and some of its strains are responsible for diseases such as pneumonia, meningitis, and intestinal infections, which can lead to death when neglected (ARBOS *et al.*, 2017).

Therefore, monitoring the microbiological quality of water from fresh and treated sewage receiving bodies is crucial for sustainable urban development such that environmental, social, economic, and public health impacts can be estimated and controlled, particularly for planning public administration.

In this context, a useful tool for estimating the concentration of *E. coli* is mathematical modeling, because experimental research has operational problems and high costs. Another advantage of mathematical modeling is its ability to adapt easily and quickly to different scenarios; among these models, the Lagrangian and Eulerian models can be used to simulate the dispersion of pollutants in rivers (OLIVEIRA, 2015).

Given the importance of achieving greater environmental control, this study aims to present a reliable manner for simulating the transport of *E. coli* in a water body. It is a useful and low-cost tool that serves as an experimental laboratory for teaching dispersion phenomena and the advection of said agents in water courses.

Despite the apparent simplicity, Partial Differential Equations (PDEs) provide a quantitative description for many central models in physical, biological, and social sciences. PDEs govern complex phenomena of motion, reaction, diffusion, equilibrium, conservation, and more. Since 1949, see Von Neumann (1949), the use of computing machines were predicted to find numerical solution of PDEs that model practical problems. Several methods were developed to solve this problems and we refer to Brandt (1977), Castro, Gomes and Stolfi (2012), Castro, Gomes and Stolfi (2016), Wesseling (2004), LeVeque (2002) and the references therein. Maybe the first numerical method for nonlinear equations was presented originally in 1928 by Courant, Friedrichs and Lewy (1967).

Turning to finite-difference schemes, as presented in the following sections, we propose solving the equation of the one-dimensional hydrodynamic model adapted from a three-dimensional model using the Crank-Nicolson method (CRANK; NICOLSON, 1947), which is implicit and stable.

## Material and method

### *The mathematical model and its discretization*

In this study, a coliform transport model was adapted from a three-dimensional hydrodynamic model used by Liu, Chan and Young (2015) for a one-dimensional model.

The parameters of advection, dispersion, and decay were considered as the first order for bacteria, because of their mortality and sedimentation during the transport process. The model is given by equation (1)

$$C_t + uC_x + vC_y + wC_z = (\mu_x C_x)_x + (\mu_y C_y)_y + (\mu_z C_z)_z - KC, \quad (1)$$

where  $u$  is the velocity in the  $x$ -direction,  $v$  the velocity in the  $y$ -direction,  $w$  the velocity in the  $z$ -direction,  $\mu_x$  the diffusion in variable  $x$ ,  $\mu_y$  the diffusion in variable  $y$ ,  $\mu_z$  the diffusion in variable  $z$ , and  $K$  is the decay coefficient of coliforms.

Some factors such as non-punctual sources and sediment resuspension may affect the concentration of coliforms in water, but this variable was not considered because of the difficulty in obtaining these parameters.

The equation used is an adaptation that considers the time and spatial variations in fecal coliform concentration, as given in equation (2)

$$C_t = -vC_x + (\mu C_x)_x - KC, \quad x \in [0, L], t \in [0, T], \quad (2)$$

where  $C(x, t)$  is the concentration of fecal coliforms,  $t$  the temporal variable,  $v$  the speed of the incompressible fluid in the  $x$ -direction, the diffusion coefficient,  $K$  the decay parameter of linear coliforms that describes the process of removing the pollutant,  $L$  the length of the stretch of stream to be analyzed that begins at the point of effluent release, and  $T$  is the defined time limit.

The initial condition used was the Dirichlet type, that is the constant is given by equation (3)

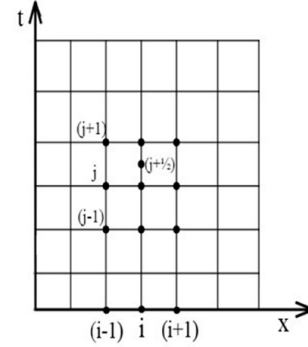
$$C(x, 0) = \begin{cases} C_0, & \text{se } x < d \\ C_L, & \text{se } x \geq d, \end{cases} \quad (3)$$

where  $C_0$  is the concentration at the launch point,  $C_L$  the natural concentration of the stream (obtained before the launch point), and  $d$  the effluent release point.

For discretization, consider  $0 \leq x \leq L$ , so the domain  $[0, L] \times [0, \infty]$  is first partitioned into sub-rectangles of the shape  $\Delta x \times \Delta t$ , where  $\Delta x = x_i - x_{i-1}$  and  $\Delta t = t_j - t_{j-1}$ , as shown in Figure 1.

Another important factor to consider in the mesh is that the Crank-Nicolson method is unconditionally stable for  $\Delta x$  and any value of  $\Delta t$ , but may present some oscillations if the ratio  $\Delta t \leq \frac{\Delta x^2}{2}$  is not applied. To avoid these oscillations, the algorithm considers a restriction in  $\Delta t$  that is widely used in computational fluid dynamic (CFD) simulations.

Figure 1 – Mesh.



Source: The authors.

Equation (2) was discretized using the Crank-Nicolson method, which is a method of finite differences, and therefore consists of approximating the derivatives of the differential equation using the differences in each corresponding subinterval of the partition. The derivatives are presented in equations (4)-(6). That is,

$$C_t = \frac{c_i^{j+1} - c_i^j}{\Delta t} \quad (4)$$

$$C_x = \frac{1}{2} \left( \frac{c_{i+1}^{j+1} - c_{i-1}^{j+1}}{2\Delta x} + \frac{c_{i+1}^j - c_{i-1}^j}{2\Delta x} \right) \quad (5)$$

$$C_{xx} = \frac{1}{2} \left( \frac{c_{i+1}^{j+1} - 2c_i^{j+1} + c_{i-1}^{j+1}}{\Delta x^2} + \frac{c_{i+1}^j - 2c_i^j + c_{i-1}^j}{\Delta x^2} \right), \quad (6)$$

where  $C(x_i, t_j) = c_i^j$ .

Replacing the derivatives in equation (2) and rearranging the terms we obtain equation (7):

$$\begin{aligned} \left( \frac{\beta}{2} - \gamma \right) c_{i+1}^{j+1} + (2\gamma + \alpha + 2) c_i^{j+1} - \left( \frac{\beta}{2} + \gamma \right) c_{i-1}^{j+1} = \\ - \left( \frac{\beta}{2} - \gamma \right) c_{i+1}^j + (-2\gamma - \alpha + 2) c_i^j + \left( \frac{\beta}{2} + \gamma \right) c_{i-1}^j, \end{aligned} \quad (7)$$

where  $\beta = \frac{v\Delta t}{\Delta x}$ ,  $\gamma = \frac{\mu\Delta t}{\Delta x^2}$  and  $\alpha = K\Delta t$ .

Therefore, rewriting equation (7), we obtain equation (8):

$$Cc_{i+1}^{j+1} + Bc_i^{j+1} - Ac_{i-1}^{j+1} = -Fc_{i+1}^j + Ec_i^j - Dc_{i-1}^j, \quad (8)$$

where  $A = \frac{\beta}{2} + \gamma$ ,  $B = 2\gamma + \alpha + 2$ ,  $C = \frac{\beta}{2} - \gamma$ ,  $D = A$ ,  $E = -2\gamma - \alpha + 2$  and  $F = C$ .

Note that  $A, B, C, D, E$  and  $F$  are coefficients of the discretized equation. After partitioning the interval  $[0, L]$ , there are  $N$  points on the  $x$ -axis, with which the solution of equation (2) is approximated.

In equation (8), by varying the  $i$  indexes from 1 to  $N$ , the following system is obtained:

$$Cc_0^{j+1} + Bc_1^{j+1} - Ac_2^{j+1} = -Fc_0^j + Ec_1^j + Dc_2^j \quad (9)$$

$$Cc_1^{j+1} + Bc_2^{j+1} - Ac_3^{j+1} = -Fc_1^j + Ec_2^j + Dc_3^j \quad (10)$$

⋮

$$Cc_{N-2}^{j+1} + Bc_{N-1}^{j+1} - Ac_N^{j+1} = -Fc_{N-2}^j + Ec_{N-1}^j + Dc_N^j. \quad (11)$$

This system, equations (9)-(11), can be written in a matrix form, and the matrix of the system is tridiagonal

$$\mathbf{MC} = \mathbf{R}, \quad (12)$$

where the coefficient matrix  $\mathbf{M}$  is a square matrix, the unknown vector  $\mathbf{C}$ , the independent term vector  $\mathbf{R}$  are given by

$$\mathbf{M} = \begin{bmatrix} B & C & 0 & \dots & 0 \\ -A & B & C & & \vdots \\ 0 & & \ddots & & 0 \\ \vdots & & -A & B & C \\ 0 & \dots & 0 & -A & B \end{bmatrix}, \quad (13)$$

$$\mathbf{C} = \begin{bmatrix} c_1^{j+1} \\ c_2^{j+1} \\ \vdots \\ c_{N-1}^{j+1} \\ c_N^{j+1} \end{bmatrix}, \quad \mathbf{R} = \begin{bmatrix} R(1) \\ R(2) \\ \vdots \\ R(N-1) \\ R(N) \end{bmatrix} \quad (14)$$

and  $R(i) = -Fc_{i-1}^j + Ec_i^j + Dc_{i+1}^j$ .

It is important to mention that using the data obtained with the initial solution at  $j = 0$ , the system, in equation (12), is resolved such that the solution is obtained at time  $t_1 = \Delta t$ . This process was repeated using the solution at  $t_1$  to obtain the solution at  $t_2 = 2\Delta t$ . In this manner, the solution to the problem given in equations (2)-(3) can be obtained at any time  $t_j = j\Delta t$ .

### Numerical implementation

This section is dedicated to explain the implementation of the numerical solution, however, it is important to mention the general advantages in seek a approximation to the analytical solution.

A major advantage of a numerical method is that a numerical solution can be obtained for problems, where an analytical solution does not exist.

The methods can provide accurate solutions in cases dealing with complex problems for which analytical solutions cannot be obtained and, in this case, it would be impossible to handle otherwise. An additional advantage is, that a numerical method only uses evaluation of standard functions and the operations: addition, subtraction, multiplication and division.

Due to the simplicity to build the code, we use Scilab 6.1.1 (SCILAB..., 2021) to implement the numerical solution to the problem given in equations (2)-(3). The analytical solution, used to compare with numerical solution was also implemented in Scilab. This open source software for numerical computation has a powerful open computing environment for scientific applications. The figures were produced using the plot function.

## Results

### The convergence order

To validate the proposed algorithm, tests were performed and compared with those in theoretical works (DIAS, 2003; SOCOLOFSKY; JIRKA, 2021). In each case, simulations with the same parameters were performed by applying the numerical convergence analysis method, which consists of comparing the performances of numerical methods in relation to the analytical solution to the same point, expressed as Galdino (2003), by equations (15) and (16)

$$C(x, t, \Delta t) \approx c(x, t) + E(x, t)\Delta t^q, \quad (15)$$

$$C(x, t, \frac{\Delta t}{2}) \approx c(x, t) + E(x, t)\frac{\Delta t^q}{2^q}. \quad (16)$$

This approximation enables the estimation of the convergence ratio of the method using the equation (17)

$$\frac{\|C(x, t, \Delta t) - c(x, t)\|_\infty}{\|C(x, t, \frac{\Delta t}{2}) - c(x, t)\|_\infty} \approx 2^q, \quad (17)$$

where  $q$  represents the order of the numerical method. The Crank-Nicolson method is a second-order numerical method, i. e.,  $q = 2$ ; thus, the ratio that must be observed in the method must approach 4 to validate the convergence of the algorithm.

Numerical experiments for pure diffusion

For the first simulation, a comparison was made between the numerical solution of given in equations (2)-(3) and exact solution of equation (18), which is a pure diffusion situation given by

$$C_t = (\mu C_x)_x. \tag{18}$$

The exact solution is given in terms of the error function by equation (19):

$$C(x,t) = C_0 \left( 1 - \operatorname{erf} \left( \frac{x}{\sqrt{4\mu t}} \right) \right). \tag{19}$$

The simulation parameters considered in problem (2)-(3) to produce Figure 2 were  $L = 5m$ ,  $\mu = 0.01m/s$ ,  $v = 0$ ,  $K = 0$ ,  $C_0 = 1$  and  $C_L = 0$ .

Figure 2 shows the curves related to the simulation with different mesh spacings. With an increase in the number of steps, a greater number of points can be seen to coincide with the analytical solution, and the same phenomenon is observed for different values of  $t$ . Therefore, the numerical solution can be considered to approach the analytical solution with the refinement of the mesh.

Applying the numerical convergence analysis method, using equation (17), the refinement of the mesh is observed by doubling the number of steps in each simulation, beginning with 25 steps up to 400 steps, for  $t = 0.25s$ .

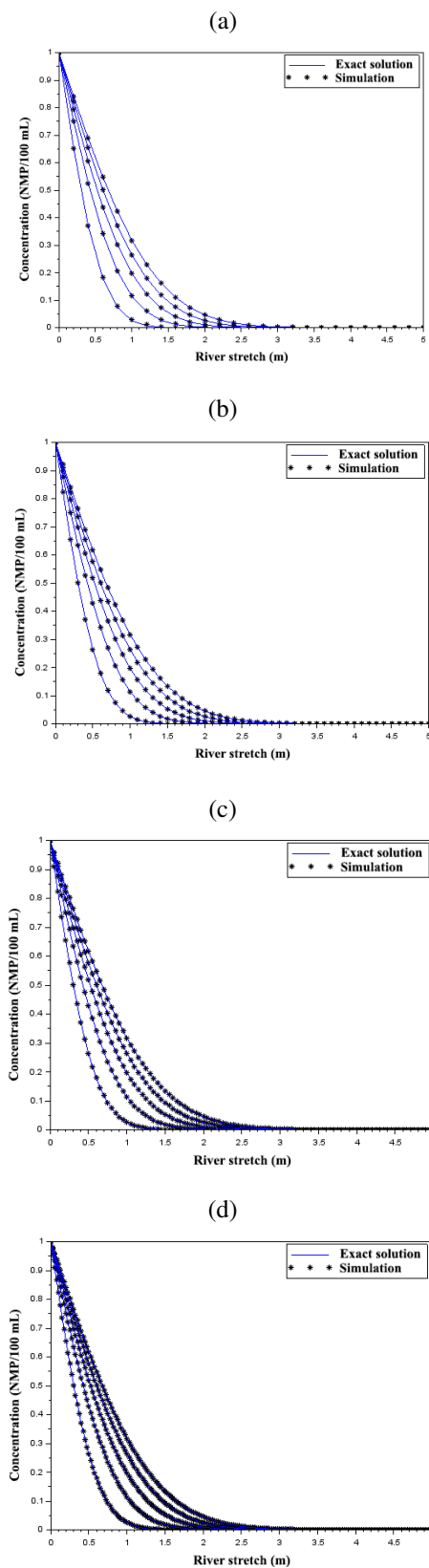
Observing the error and ratio between these errors, according to Table 1, implies the convergence of the method, because, for each refinement, the ratio approaches 4; thus, the method for pure diffusion can be validated.

**Table 1** – Validation data of the algorithm with the error mesh parameters for  $t = 1s$  for pure diffusion.

Steps	$\Delta x$	$\Delta t$	$E = \ C - c\ _\infty$	Reason
25	0.2	0.02	0.021032	
50	0.1	0.005	0.005258	3.999856
100	0.05	0.00125	0.001314	4.002854
200	0.025	0.0003125	0.000328	4.000585
400	0.0125	0.000078125	0.0000821	4.000006

Source: The author.

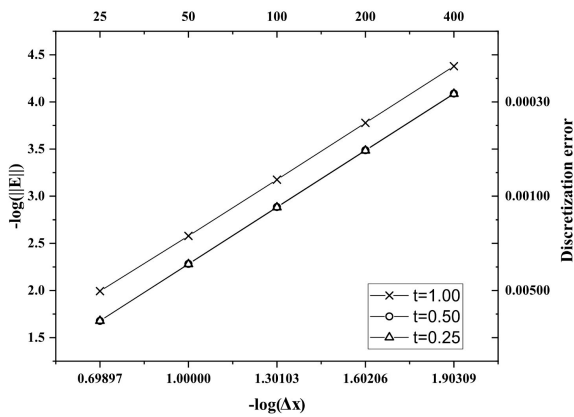
**Figure 2** – Comparing numerical and exact solutions with a) 25 steps, b) 50 steps, c) 100 steps, and d) 200 steps in space and at times  $t = 20, 40, 60, 80,$  and  $100s$ .



Source: The author.

For Figure 3, the same analysis was performed, but using times  $t = 0.25s$  and  $0.50s$ , to verify that the method requires more time to converge at longer time intervals. By analyzing the graph, the algorithm is evidently more accurate if a longer time interval is considered, because the error for time  $t = 0.25s$  is on a scale of  $1.0 \times 10^{-4}$  for a step number equal to 400, and for the same step number for  $t = 1s$ , the error is in a scale of  $1.0 \times 10^{-5}$ .

**Figure 3** – Error ratio with an increased number of steps at different time intervals for pure diffusion.



Source: The author.

*Numerical experiments for diffusion-advection*

The simulation parameters considered in problem (2)-(3) to produce Figure 4 were  $L = 5m$ ,  $\mu = 0.1m/s$ ,  $\nu = 0.5m/s$ ,  $K = 0$ ,  $C_0 = 1$  and  $C_L = 0$ . In the simulation, the advective part of the differential equation was considered, which was responsible for the transport of the matrix (coliforms) because the presence of current in the stream was considered.

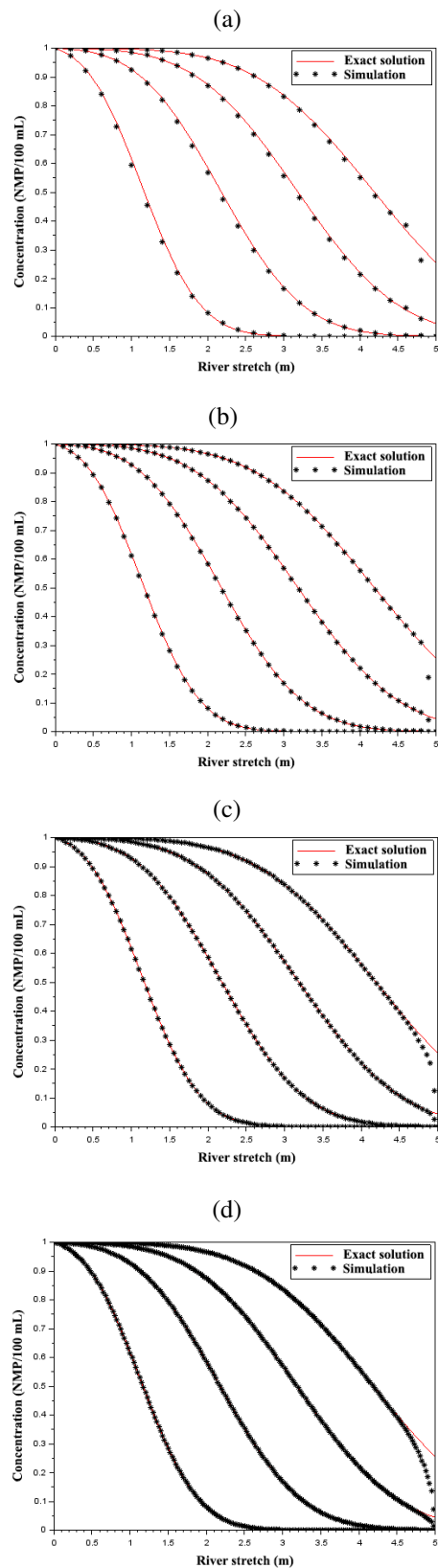
In Figure 4, the graphs of the analytical solution, equation (20), are compared with the graph of the numerical solution, which was generated in different numbers of steps. The diffusion-advection equation is

$$C_t + \nu C_x = (\mu C_x)_x. \tag{20}$$

From Figure 4, the greater the number of steps, the closer the numerical simulation is to the analytical solution.

In Figure 4, a deviation of the points is noticed when approaching the end of the stretch  $x = L$ . This is because of the difference in the contour conditions imposed on the algorithm and exact solution, but the same does not affect the efficiency of the algorithm compared with the exact solution.

**Figure 4** – Refining comparison of numerical solutions with the exact solution, with parameters a) 25 steps, b) 50 steps, c) 100 steps, and d) 200 steps in space and at times  $t = 2, 4, 6,$  and  $8s$  for the diffusion-advection equation.



Source: The author.

Table 2 lists the ratio of the errors of two consecutive refinements. For comparison, the number of sample points is always doubled to validate the stability and convergence of the method. As observed when the mesh size is reduced, the ratio approaches four, confirming that the method is of order 4, thereby validating the algorithm for equation (20).

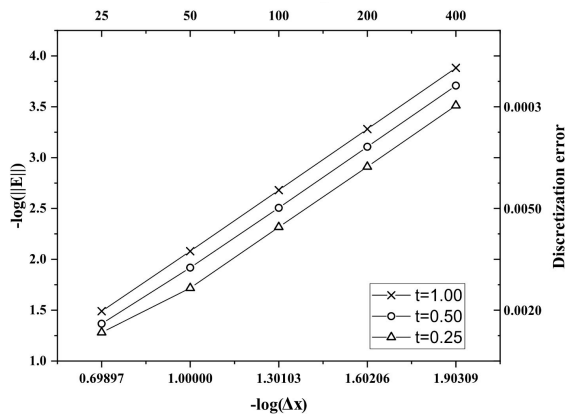
**Table 2** – Validation data of the algorithm with the error mesh parameters for  $t = 1s$  for diffusion-advection equation.

Steps	$\Delta x$	$\Delta t$	$E = \ C - c\ _\infty$	Reason
25	0.2	0.02	0.032354	
50	0.1	0.005	0.008322	3.887614
100	0.05	0.00125	0.002089	3.984201
200	0.025	0.0003125	0.000524	3.983979
400	0.0125	0.000078125	0.000131	3.999237

Source: The author.

To analyze the convergence of the algorithm for shorter time intervals, Figure 5 was generated, which demonstrates that, at shorter time intervals, the algorithm did not present a large difference in error, remaining at ( $t = 1.0, 0.5,$  and  $0.25s$ ) on the same scale of a  $1.0 \times 10^{-4}$  error.

**Figure 5** – Error ratio with an increased number of steps at different time intervals for diffusion-advection.



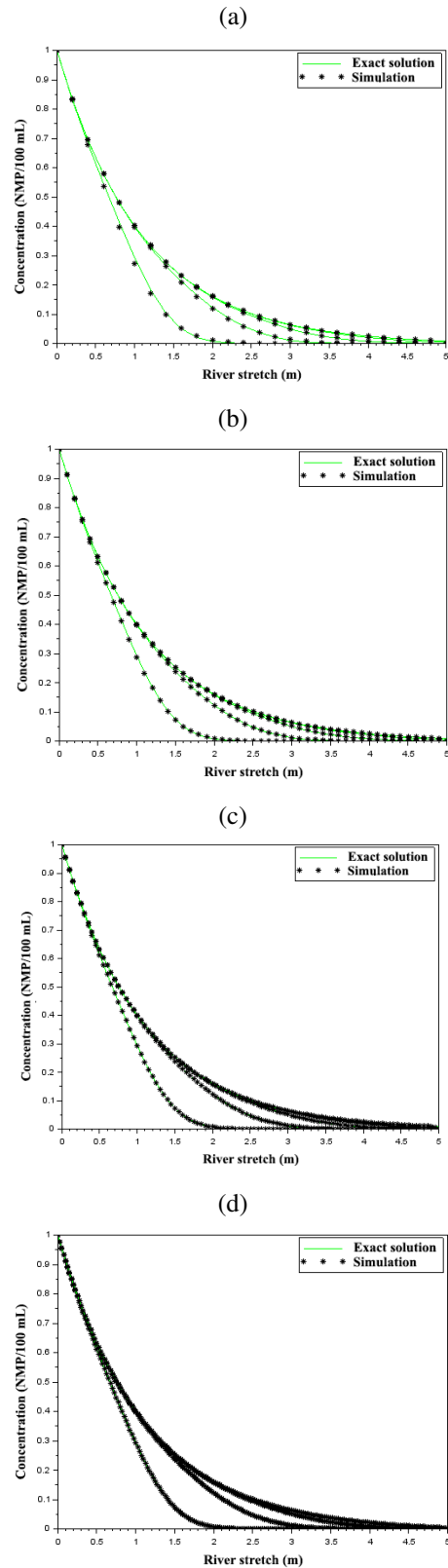
Source: The author.

*Numerical experiments for diffusion-advection and decay*

The simulation parameters considered in problem (2)-(3) to produce Figure 6 were  $L = 5m$ ,  $\mu = 0.01m/s$ ,  $v = 0.5m/s$ ,  $K = 1m/s$ ,  $C_0 = 1$  and  $C_L = 0$ . The simulation considered beyond the advective part of the previous section; the coliform decay was considered, which is the natural death of bacterial cells that sink to the bottom of the stream.

Figure 6 shows that the numerical solution approaches the analytical solution by increasing the number of steps in each simulation.

**Figure 6** – Refining the mesh of the simulated model with the exact solution, with parameters a) 25 steps, b) 50 steps, c) 100 steps, and d) 200 steps in space and at times  $t = 1, 2, 3, 4$  and  $5s$  for diffusion-advection with decay.



Source: The author.

Another point to note, in Figure 6, is that comparing the results with the problems of pure diffusion and diffusion-advection, a decrease in concentration is observed in a shorter time, confirming the effect of decay on the capacity of self-purification of water through theoretical simulation.

As in the previous sections, a numerical convergence analysis was performed. By observing the relationship between the overall error and mesh decrease, and the higher the number of steps, the smaller the overall error seemed to be. In addition, it presented a ratio close to four, confirming that the numerical method is second-order. Table 3 presents the results.

**Table 3** – Validation data of the algorithm with the error mesh parameters for  $t = 1s$  for diffusion-advection and decay equation.

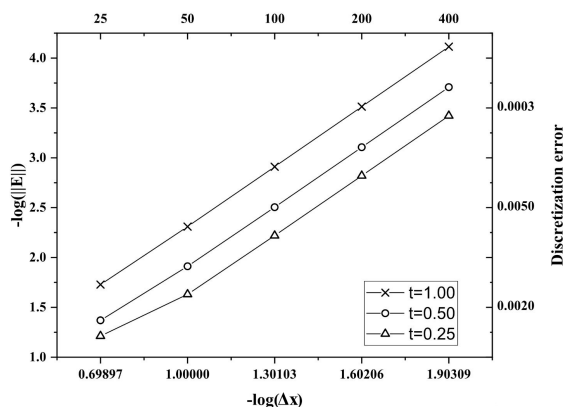
Steps	$\Delta x$	$\Delta t$	$E = \ C - c\ _{\infty}$	Reason
25	0.2	0.02	0.0186993	
50	0.1	0.005	0.0049043	3.812838
100	0.05	0.00125	0.0012286	3.991779
200	0.025	0.0003125	0.0003075	3.995447
400	0.0125	0.000078125	0.0000769	3.9987

Source: The author.

To verify the behavior of the method in shorter time intervals, error analyses were conducted for times  $t = 0.5s$  and  $0.25s$ . The longer the simulation time, the higher the accuracy of the method was observed to be, and, in this analysis, a difference was verified in the error scale of 10 times.

Therefore, in Figure 7, at time  $t = 1s$  and 400 steps, the error is on a scale of  $1.0 \times 10^{-5}$ , and, for time  $t = 0.25s$  with the same step number, an error scale of  $1.0 \times 10^{-4}$ , validating the algorithm for longer time intervals.

**Figure 7** – Error ratio with an increased number of steps at different time intervals for diffusion-advection and decay.



Source: The author.

## Conclusion

The mathematical model was based on theoretical models from the literature. The mathematical model was solved using the Crank-Nicolson finite differences method because it is stable in space and time for second-order EDPs; the mathematical solution was simulated and compared to models from the literature to validate the developed algorithm, which was validated by refining the mesh and overall error of the models.

The simulated model presented results similar to those of the literature, thereby validating the algorithm. Therefore, the present work and mathematical simulations are satisfactory compared with the literature.

## Acknowledgments

This work was carried out with the support of the National Council for Scientific and Technological Development - CNPq - Brazil. The authors would like to thank CAPES (Coordenação de Aperfeiçoamento de Pessoal de Nível Superior - Coordination for the Improvement of Higher Education Personnel - Brazil) (Financing Code 001 CAPES) and PROPESQ; and the Federal University of Tocantins for financial assistance (Edital 40/2021). The third and fourth authors thank the Tocantins Research Support Foundation - FAPT for the financial support. We would like to thank Editage (www.editage.com) for English language editing.

## References

ARBOS, K. A. *et al.* Qualidade microbiológica da água para consumo humano no loteamento Nova Esperança: Litoral Sul da Paraíba e sua importância para a Saúde Pública. *Revista de Ciências da Saúde Nova Esperança*, Gramame, v. 15, n. 2, p. 50-56, 2017. DOI: <https://doi.org/10.17695/revcsnevol15n2p50-56>.

BALDOCHI, M. A. *Utilização do modelo QUAL2E como apoio ao gerenciamento da qualidade das águas da bacia do córrego dos Bagres*. 2002. Dissertation (Master's) - Universidade de São Paulo, São Paulo, 2002.

BASSANEZI, R. *Ensino-aprendizagem com Modelagem matemática*. São Paulo: Contexto, 2002.



- BRANDT, A. Multi-level adaptive solutions to boundary-value problems. *Mathematics of Computation*, Providence, v. 31, p. 333-390, 1977. DOI: <https://doi.org/10.2307/2006422>.
- CASTRO, D. A.; GOMES, S. M.; STOLFI, J. An adaptive multiresolution method on dyadic grids: application to transport equations. *Journal of Computational and Applied Mathematics*, Antwerpen, v. 236, n. 15, p. 3636-3646, 2012. DOI: <https://doi.org/10.1016/j.cam.2011.05.044>.
- CASTRO, D. A.; GOMES, S. M.; STOLFI, J. High-order adaptive finite-volume schemes in the context of multiresolution analysis for dyadic grids. *Computational and Applied Mathematics*, Petrópolis, v. 35, p. 1-16, 2016. DOI: <https://doi.org/10.1007/s40314-014-0159-2>.
- CLILVERD, H. M.; THOMPSON, J. R.; HEPPELL, C. M.; SAYER, C. D.; AXMACHER, J. C. Coupled hydrological/hydraulic modelling of river restoration impacts and floodplain hydrodynamics. *River Research and Applications*, Chichester, v. 32, n. 9, p. 1927-1948, 2016. DOI: <https://doi.org/10.1002/rra.3036>.
- COURANT, R.; FRIEDRICHS, K.; LEWY, H. On the partial difference equations of mathematical physics. *IBM Journal*, Armonk, v. 11, n. 2, p. 215-234, 1967.
- CRANK, J.; NICOLSON, P. A practical method for numerical evaluation of solutions of partial differential equations of the heat-conduction type. *Mathematical Proceedings of the Cambridge Philosophical Society*, Cambridge, v. 43, n. 1, p. 50-67, 1947. DOI: <https://doi.org/10.1017/S0305004100023197>.
- DIAS, N. Obtenção de uma solução analítica da equação de difusão-advectação com decaimento de 1ª ordem pelo método da transformação de similaridade generalizada. *Revista Brasileira de Recursos Hídricos*, Porto Alegre, v. 8, p. 181-188, 2003.
- GALDINO, A. *A técnica do super-passo na resolução numérica de equações diferenciais parciais parabólicas*. 2006. Thesis (Doctor) - Universidade de São Paulo, São Paulo, 2006.
- JOBIM, G. S. *Dispersão de poluentes: simulação numérica do Lago Guaíba*. 2012. Dissertation (Master's) - Universidade Federal do Rio Grande do Sul, Porto Alegre, 2012.
- LEVEQUE, R. J. *Finite volume methods for hyperbolic problems*. Cambridge: Cambridge University Press, 2002. (Cambridge texts in Applied Mathematics). DOI: <https://doi.org/10.1017/CBO9780511791253>.
- YOUNG LIU, W.-C.; CHAN, W.-T.; YOUNG, C.-C. Modeling fecal coliform contamination in a tidal Danshuei River estuarine system. *Science of The Total Environment*, Amsterdam, v. 502, p. 632-640, 2015. DOI: <https://doi.org/10.1016/j.scitotenv.2014.09.065>.
- OLIVEIRA, R. E. *Dispersão de contaminantes em rios e canais através do método GILTT*. 2015. Dissertation (Master's) - Universidade Federal de Pelotas, Pelotas, 2015.
- OSIŃSKA, A.; KORZENIEWSKA, E.; HARNISZ, M.; NIESTEŃSKI, S. The prevalence and characterization of antibiotic-resistant and virulent Escherichia coli strains in the municipal wastewater system and their environmental fate. *Science of The Total Environment*, Amsterdam, v. 577, p. 367-375, 2016. DOI: <https://doi.org/10.1016/j.scitotenv.2016.10.203>
- SCILAB 6.1.1. Rungis: Scilab, 2021. 1 software. Available from: <https://www.scilab.org/>. Access: July 25, 2021.
- SEFFRIN, G. F. F. *Simulação atual e previsão futura da qualidade das águas do rio Ibicuí utilizando o modelo QUAL2E*. 2001. Thesis (Doctor) - Universidade Federal de Santa Maria, Santa Maria, 2001.
- SOCOLOFSKY, S. A.; JIRKA, G. H. *Environmental fluid mechanics. part I: mass transfer and diffusion*. 2nd ed. Karlsruhe: Institut für Hydromechanik, 2002. (Engineering-lectures). Available from: <https://publikationen.bibliothek.kit.edu/1542004>. Access: July 25, 2021.

TUNDISI, J. G. Recursos hídricos no futuro: problemas e soluções. *Estudos Avançados*, São Paulo, v. 22, p. 7-16, 2008.

WESSELING, P. *An introduction to multigrid methods*. Philadelphia: R.T. Edwards, 2004.

VON NEUMANN, J. A letter to V. Bush. In: REDEI, M. (ed.). *John von Neumann: selected letters*. London: American Mathematical Society, 1949. p. 103-111. (History of Mathematics, v. 27).

*Received: Sept. 22, 2022*  
*Accepted: Nov. 9, 2022*  
*Published: Nov. 19, 2022*